https://doi.org/10.5194/bg-2020-243
Preprint. Discussion started: 24 July 2020

Biogeosciences Discussions

Impacts of biogenic polyunsaturated aldehydes on metabolism and community composition of particle-attached bacteria in coastal hypoxia

Zhengchao Wu[1,2], Qian P. Li[1,2,3,]*, Zaiming Ge[1,3], Bangqin Huang[4], Chunming Dong[5]

[1]State Key Laboratory of Tropical Oceanography, South China Sea Institute of Oceanology, Chinese Academy of Sciences, Guangzhou, China

[2]Southern Marine Science and Engineering Guangdong Laboratory, Guangzhou, China

[3]College of Marine Science, University of the Chinese Academy of Sciences, Beijing, China

[4]Fujian Provincial Key Laboratory of Coastal Ecology and Environmental Studies, State Key Laboratory of Marine Environmental Science, Xiamen University, Xiamen, China

[5]Key Laboratory of Marine Genetic Resources, Third Institute of Oceanography, MNR, Xiamen, China

**Correspondence to*: Qian Li (qianli@scsio.ac.cn)

Abstract. Eutrophication-driven coastal hypoxia is of great interest recently, though its mechanisms are not fully understood. Here, we showed elevated concentrations of particulate and dissolved polyunsaturated aldehydes (PUAs) associated with the hypoxic waters meanly dominated by particle-attached bacteria (PAB) in the bottom water of a salt-wedge estuary. Particle-adsorbed PUAs of ~10 micromoles per liter particle in the hypoxic waters were directly quantified for the first time using large-volume-filtration followed with on-site derivation and extraction of the adsorbed PUAs. PUAs-amended incubation experiments for PAB retrieved from the low-oxygen waters were also performed to explore the impacts of PUAs on the growth and metabolism of PAB and associated oxygen utilization. We found an increase in cell growth of PAB in response to low-dose PUAs (1 μmol L^{-1}) but an enhanced cell-specific metabolic activity in response to high-dose PUAs (100 μmol L^{-1}) including bacterial respiration and production. Improved cell-specific metabolism of PAB in response to high-dose PUAs was also accompanied by a significant shift of PAB community structure with increased dominance of genus *Alteromonas* within the Gammaproteobacteria. We

https://doi.org/10.5194/bg-2020-243
Preprint. Discussion started: 24 July 2020

thus conclude that a high PUAs concentration within the bottom layer may be important for species such as *Alteromonas* to regulate PAB community structure and lead to the enhancement of oxygen utilization during the degradation of particulate organic matters and thus contribute to the formation of coastal hypoxia. These findings are potentially important for coastal systems with large river inputs, intense phytoplankton blooms driven by eutrophication, as well as strong hypoxia developed below the salt-wedge front.

https://doi.org/10.5194/bg-2020-243
Preprint. Discussion started: 24 July 2020


Biogeosciences Discussions Open Access EGU

1. Introduction

Coastal hypoxia, defined as dissolved oxygen levels < 62.5 μmol kg^{-1}, has become a worldwide problem in recent decades (Diaz and Rosenberg 2008; Helm et al., 2011). It could affect diverse life processes from genes to ecosystems, resulting in the spatial and temporal change of marine food-web structures (Breitburg et al., 2018). Coastal deoxygenation was also tightly coupled with other global issues, such as ocean warming and acidification (Doney et al., 2012). Formation and maintenance of eutrophication-derived hypoxia in the coastal waters should reflect the interaction between physical and biogeochemical processes (Kemp et al., 2009). Generally, seasonal hypoxia occurs in the coastal ocean when strong oxygen sinks are coupled with restricted resupply during periods of strong density stratification. Termination of the event occurs with oxygen resupply when stratification is eroded by vertical mixing (Fennel and Testa, 2019).

Bacterial respiration accounts for the largest portion of aquatic oxygen consumption and is thus pivotal for the development of hypoxia and oxygen minimum zones (Williams and del Giorgio, 2005; Diaz and Rosenberg, 2008). Particle-attached bacteria (PAB) are known to be more abundant than free-living bacteria (FLB) with higher metabolic activity in coastal waters and may play an important role in the carbon cycle through organic matter remineralization (Garneau et al., 2009). An increased contribution of PAB to respiration relative to FLB can occur during the development of coastal phytoplankton bloom (Huang et al., 2018). In the Columbia River estuary, the particle-attached bacterial activity could be 10-100 folds higher than that of its free-living counterparts leading to its dominant role in organic detritus remineralization (Crump et al, 1998). Therefore, it is crucial to assess the respiration process associated with PAB and its controlling factors, in order to fully understand oxygen utilization in the hypoxic area with an intense supply of particulate organic matters.

There is an increasing area of seasonal hypoxia in the nearshore bottom waters of the Pearl River Estuary (PRE) and the adjacent northern South China Sea (NSCS) (Yin et al., 2004; Zhang and Li 2010; Su et al., 2017). The hypoxia is generally developed at the bottom of the salt-wedge where downward mixing of oxygen is restrained due to increased stratification and where there is an accumulation of

https://doi.org/10.5194/bg-2020-243
Preprint. Discussion started: 24 July 2020

eutrophication-derived organic matter due to flow convergence driven by local hydrodynamics (Lu et al., 2018). Besides physical and biogeochemical conditions, aerobic respiration is believed the ultimate cause of hypoxia here (Su et al., 2017). Thus, microbial respiration had been strongly related to the consumption of bulk dissolved organic carbon in the PRE hypoxia (He et al., 2014). Phytoplankton-derived polyunsaturated aldehydes (PUAs) are known to affect marine microorganisms over various trophic levels (Ribalet et al., 2008; Ianora and Miralto, 2010; Edwards et al., 2015; Franzè et al., 2018). A nanomolar level of PUAs recently reported in the coastal waters outside the PRE was hypothesized to affect oxygen depletion by controlling microbial utilization of organic matters in the bottom waters (Wu and Li, 2016), while the actual role of PUAs on bacterial metabolism within the bottom hypoxia remains largely unexplored.

In this study, we focus on the particle-attached bacteria within the core of the hypoxic waters by exploring the linkage between PUAs and bacterial oxygen utilization on the suspended organic particles. Particle-adsorbed PUAs within the hypoxic waters were directly quantified for the first time based on large-volume filtration and on-site derivation and extraction of the adsorbed PUAs. Field PUAs-amended incubation experiments were conducted for PAB retrieved from the low-oxygen waters to assess their responses including bacterial abundance, respiration, production, and community composition to the treatments of different doses of PUAs. An additional experiment was also performed to verify that the observed effects of PUAs on PAB were not due to an increase of carbon source. By synthesizing these field experimental results with the change of water-column biogeochemistry of the hypoxic zone, we explore the underlying mechanism for particle-adsorbed PUAs influencing on community structure and metabolism of PAB in the low-oxygen waters, as well as its contribution to coastal deoxygenation of the NSCS shelf-sea.

2. Methods

2.1 Descriptions of field campaigns and sampling approaches

Field survey cruises were conducted in the PRE and the adjacent NSCS during June 17th-28th, 2016 and

https://doi.org/10.5194/bg-2020-243
Preprint. Discussion started: 24 July 2020

June 18st-June 2nd, 2019 (Figure 1). Briefly, vertical profiles of temperature, salinity, dissolved oxygen, and turbidity were acquired from a Seabird 911 rosette sampling system. The oxygen sensor data were corrected by field titration measurements during the cruise. Water samples at various depths were collected using 6 or 12 liter (12 or 24 positions) Niskin bottles attached to the Rosette sampler. Surface water samples were collected at ~1m or 5 m depth, while bottom water samples were obtained at depths ~4 m above the bottom. Chlorophyll-*a* (Chl-*a*) samples were taken at all depths at all stations and nutrients were also sampled except at a few discrete stations. For the 2016 cruise, samples for pPUAs were collected at all depths close to station X1 (Figure 1A). During the summer of 2019, vertical profiles of pPUAs and dPUAs were determined at Y1 in the hypoxic zone and Y2 outside the hypoxic zone with field PUAs-amended experiments conducted at Y1 (Figure 1B)

2.2 Determination of chlorophyll-*a*, dissolved nutrients

For Chl-*a* analyses, 500 mL of water sample was gently filtered through a 0.7 μm Whatman GF/F filter. The filter was then wrapped by a piece of aluminum foil and stored at -20 °C on board. Chl-*a* was extracted at 4 ºC in the dark for 24 h using 5 mL of 90% acetone. After centrifuged at 4000 rpm for 10 min, Chl-*a* was measured using a standard fluorometric method with a Turner Designs fluorometer (Parsons et al., 1984). Water samples for nutrients were filtered through 0.45 μm Nucleopore filters and stored at -20 °C. Nutrient concentrations including nitrate plus nitrite, phosphate, and silicate were measured using a segmented-flow nutrient autoanalyzer (Seal AA3, Bran-Luebbe, GmbH).

2.3 Sampling and measurements of particulate and dissolved PUAs in one-liter seawater

We used a similar protocol of Wu and Li (2016) for pPUAs and dPUAs collection, pretreatment, and determination. Briefly, 2-4 liters of water sample went through a GF/C filtration with both the filter and the filtrate collected separately. The filter was rinsed by the derivative solution with the suspended particle samples collected in a glass vial. After adding internal standard, the samples in the vial were frozen and

https://doi.org/10.5194/bg-2020-243
Preprint. Discussion started: 24 July 2020

106 thawed three times to mechanically break the cells for pPUAs. The filtrate from the GF/C filtration was
107 also added with internal standard and transferred to a C18 solid-phase extraction cartridge. The elute from
108 the cartridge with the derivative solution was saved in a glass vial for dPUAs. Both pPUAs and dPUAs
109 samples were frozen and stored at -20 ºC.
110 In the laboratory, the pPUAs sample was thawed with the organic phase extracted. After the solvent
111 was evaporated with the sample concentrated and re-dissolved in hexane, pPUAs was determined using gas
112 chromatography and mass spectrometry (Agilent Technologies Inc., USA). Standards series were prepared
113 by adding certain amounts of three major PUAs to the derivative solution and went through the same
114 pretreatment and extraction steps as samples. Derivatives of dPUAs were extracted and measured by
115 similar methods as pPUAs, except that the calibration curves of dPUAs were constructed separately. The
116 units of pPUAs and dPUAs are nmol L^{-1} (nmol PUA in one-liter seawater).
117
118 **2.4 Particle collections by large-volume filtrations in hypoxia waters.**
119 Large volumes (~300 L) of the middle (12m) and the bottom (25m) waters at a station within the hypoxia
120 zone were collected by Niskin bottles and quickly filtered through a sterile fabric screen (25 μm filter) on a
121 disk filter equipped with a peristaltic pump to qualitatively obtain particles of >25 μm. The particles were
122 gently back-flushed three times off the fabric screen using particle-free seawater (obtained using a 0.2 μm
123 filtration of the same local seawater) into a sterile 50-mL sampling tube.
124 The volume of total particles from large-volume-filtration was measured as follows: The collected
125 particle in the 50 mL tube was centrifuged for one minute at a speed of 3000 revolutions per minute (r.p.m)
126 with supernatant removed (Hmelo et al., 2011). The particle sample was resuspended as slurry and
127 transferred into a sterile 5 mL graduated centrifuge tube. The sample was centrifuged again by the same
128 centrifuging speed with the final volume of the total particles recorded. The unit for the total particles is
129 mL.

https://doi.org/10.5194/bg-2020-243
Preprint. Discussion started: 24 July 2020

All the particles were transferred back to the sterile 50 mL centrifuge tube with 0.2-μm-filtered seawater, which was used for subsequent measurements of particle-adsorbed PUAs as well as for PUAs-amended incubation experiments of particle-attached bacteria.

2.5 Measurements of particle-adsorbed PUAs

After gently shaking, 3 mL of sample in the 50 mL sampling tube (see section 2.4) was used for the analyses of particle-adsorbed PUAs concentration (two replicates) according to the procedure shown in Figure 2. The sample was transferred to 50 mL centrifuge tubes for PUAs derivatization on board. An internal standard of benzaldehyde was added to obtain a final concentration of 10 μM. The aldehydes in the samples were derivatized by the addition of O-(2,3,4,5,6-pentafluorobenzyl) hydroxylamine hydrochloride solution in deionized water (*p*H=7.5). The reaction was performed at room temperature for 15 min (shaking slightly for mix every 5 min). Then 2 mL sulfuric acid (0.1%) solution was added to a final concentration of 0.01% acid (*p*H of 2-3) to avoid new PUAs induced by enzymatic cascade reactions. The derivate samples were subsequently sonicated for 3 min before the addition of 20 mL hexane, and the upper organic phase of the extraction was transferred to a clean tube and stored at -20 °C.

Upon returning to the laboratory, the adsorbed PUAs on these particles (undisrupted PUAs) were determined with the same methods as those for the disrupted pPUAs (freeze-thaw methods to include the portion of PUAs eventually produced as cells die, Wu and Li 2016). A separate calibration curve was made for the undisrupted PUAs derivates. A standard series of heptadienal, octadienal, and decadienal (0, 0.1, 0.5, 1.0, 2.5, 5.0, 10.0, 25.0 nmol L^{-1}) was prepared before each analysis by diluting a relevant amount of the PUA stock solution (methanolic solution) with deionized water. These standard solutions were processed through all the same experimental steps as those mentioned above for derivation, extraction, and measurement of the undisrupted PUAs sample. The unit for the undisrupted PUAs is nmol.

The final particle-adsorbed PUAs in one-liter particles, defined as PUAs [μmol $L^{-1}{}_{particle}$], would equal to the moles of particle-adsorbed PUAs (nmol) divided by the volume of particles (mL).

https://doi.org/10.5194/bg-2020-243
Preprint. Discussion started: 24 July 2020

155

156 **2.6 Incubation of particle-attached bacteria with PUAs treatments.**

157 Impact of PUAs on microbial growth and metabolisms in the hypoxia zone was assessed by field
158 incubation of particle-attached bacteria collected from large-volume filtration with direct additions of low
159 or high doses of PUAs (1 or 100 μmol L^{-1}) on June, 29th, 2019 (Figure 2).

160 A sample volume of ~32 mL in the centrifuge tube (section 2.4) was transferred to a clean Nalgene
161 bottle before being diluted by particle-free seawater to a final volume of 4 L. About 3.2 L of the sample
162 solution was transferred into four clean 1-L Nalgene bottles (each with 800 mL). One 1-L bottle was used
163 for determining the initial conditions: after gentle shaking, the solution was transferred into six biological
164 oxygen demand (BOD) bottles with three for initial oxygen concentration (fixed immediately by Winkler
165 reagents) and the other three for initial bacterial abundance, production, and community structure. The
166 other three 1-L bottles were used for three different treatments: the first one served as the control with the
167 addition of 400 μL methanol, the second one with 400 μL low-dose PUAs solution, and the third one with
168 400 μL high-dose PUAs solution (Table 1). The solution in each of the three treatments (1-L bottles) was
169 transferred to six parallel replicates by 60-mL BOD bottles. These BOD bottles were incubated at *in situ*
170 temperature in the dark for 12 hours. At the end of each incubation, three of the six BOD bottles were used
171 for determining the final oxygen concentrations with the other three for the final bacterial abundance,
172 production, and community structure.

173 To test the possibility of PUAs as carbon sources for bacterial utilization, a minimal medium was
174 prepared with only sterile artificial seawater but not any organic carbons (Dyksterhouse et al., 1995). A
175 volume of 375 μL sample (from the above 4 L sample solution) was inoculated in the minimal medium
176 amended with heptadienal in a final concentration of about 0.2 mmol L^{-1}. For comparisons, the same
177 amount of sample was also inoculated in the minimal medium (75 mL) amended with an alkane mixture
178 (ALK, n-pentadecane and n-heptadecane) at a final concentration of 0.25 g L^{-1}, or with a mixture of
179 polycyclic aromatic hydrocarbons (PAH, naphthalene and phenanthrene) at a final concentration of 200

https://doi.org/10.5194/bg-2020-243
Preprint. Discussion started: 24 July 2020

ppm. Significant turbidity changes in the cell culture bottle over incubation time will be observed if there is a carbon source for bacterial growth.

2.7 Measurements of bacteria-related parameters

(1) Bacterial abundance

At the end of the 12-h incubation period, a 2 mL sample from each BOD bottle was preserved in 0.5% glutaraldehyde. The fixation lasted for half of an hour at room temperature before being frozen in liquid N_2 and stored in a −80 °C freezer. In the laboratory, the samples were performed through a previously published procedure for detaching particle-attached bacteria (Lunau et al., 2005), which had been proved effective for samples with high particle concentrations. To account for detaching bacteria due to breaking up particles, 0.2 mL pure methanol was added to the 2 mL sample and vortexed. The sample was then incubated in an ultrasonic bath (35 kHz, 2 x 320W per period) at 35 °C for 15 min. Subsequently, the tube sample was filtered with 50 μm-filter to remove large detrital particles. The filtrate samples for surface-associated bacteria cells were diluted by 5-10 folds using TE buffer solution and stained with 0.01% SYBR Green I in the dark at room temperature for 40 min. With the addition of 1-μm beads, bacterial abundance (BA) of the samples was counted by a flow cytometer (Beckman Coulter CytoFlex S) with bacteria detected on a plot of green fluorescence versus side scatter.

(2) Bacterial respiration

Dissolved oxygen was determined by a high-precision Winkler titration apparatus (Metrohm-848, Switzerland) based on the classic method (Oudot et al., 1988). Bacterial respiration (BR) was calculated based on the oxygen decline during the 12-h incubation and was converted to carbon units with the respiratory quotient assumed equal to 1 (Hopkinson, 1985).

(3) Bacterial production

https://doi.org/10.5194/bg-2020-243
Preprint. Discussion started: 24 July 2020

Bacterial production (BP) was determined using a modified protocol of ^{3}H-leucine incorporation method (Kirchman, 1993). Four 1.8-mL aliquots of the sample were collected by pipet from each BOD incubation and added to 2-mL sterile microcentrifuge tubes, which were incubated with ^{3}H-leucine (in a final concentration of 4.65 μmol Leu L^{-1}, Perkin Elmer, USA). One tube served as the control was fixed by adding 100% trichloroacetic acid (TCA) immediately. The other three were terminated with TCA at the end of the 2-h dark incubation. Samples were filtered onto 0.2-μm polycarbonate filters and then rinsed twice with 5% TCA and three times with 80% ethanol before being stored at −80 °C. In the laboratory, the filters were transferred to scintillation vials with 5 mL of Ultima Gold scintillation cocktail. The incorporated ^{3}H was determined using a Tri-Carb 2800TR liquid scintillation counter. Bacterial production was calculated with the previous published leucine-to-carbon empirical conversion factors of 0.37 kg C mol $leucine^{-1}$ in the study area (Wang et al., 2014). Bacterial carbon demand (BCD) was calculated as the sum of BP and BR. Bacterial growth efficiency (BGE) was equated to BP/BCD.

(4) Bacterial community structure

At the end of incubation, DNA sample was obtained by filtering 30 mL of each BOD water via a 0.22-μm Millipore filter, which was preserved in a cryovial with the DNA protector buffer and stored at -80 °C. DNA was extracted using the DNeasy PowerWater Kit with genomic amplification by Polymerase Chain Reaction (PCR). Basically, the V3 and V4 fragments of bacterial 16S rRNA were amplified at 94 °C for 2 min and followed by 27 cycles of amplification (94 °C for 30 s, 55° C for 30 s, and 72 °C for 60 s) before a final step of 72 °C for 10 min. Primers for amplification included 341F (CCTACGGGNGGCWGCAG) and 805R (GACTACHVGGGTATCTAATCC). Reactions were performed in 10-μL mixture containing 1 μL Toptaq Buffer, 0.8 μL dNTPs, 10 μM primers, 0.2 μL Taq DNA polymerase, and 1 μL Template DNA. Three parallel amplification products for each sample were purified by an equal volume of AMpure XP magnetic beads. Sample libraries were pooled in equimolar and paired-end sequenced (2×250 bp) on an Illumina MiSeq platform.

https://doi.org/10.5194/bg-2020-243
Preprint. Discussion started: 24 July 2020

High-quality sequencing data was obtained by filtering on the original off-line data. Briefly, the raw data was pre-processed using TrimGalore to remove reads with qualities of less than 20 and FLASH2 to merge paired-end reads. In addition, the data were also processed using Usearch to remove reads with a total base error rate of greater than 2 and short reads with a length of less than 100 bp and using Mothur to remove reads containing more than 6 bp of N bases. We further used UPARSE to remove the singleton sequence to reduce the redundant calculation during the data processing. Sequences with similarity greater than 97% were clustered into the same operational taxonomic units (OTUs). R software was used for community composition analysis.

2.8 Statistical Analysis

All statistical analyses were performed using the statistical software SPSS (Version 13.0, SPSS Inc., Chicago, IL, USA). A student's t-test with a 2-tailed hypothesis was used when comparing PUAs-amended treatments with the control or comparing stations inside and outside the hypoxic zone, with the null hypothesis being rejected if the probability (p) is less than 0.05. We consider p of <0.05 as significant and p of <0.01 as strong significant. Ocean Data View with the extrapolation model "DIVA Gridding" method was used to contour the spatial distributions of physical and biogeochemical parameters.

3. Results

3.1 Characteristics of hydrography, biogeochemistry, and bulk bacteria community in the hypoxic zone

During our study periods, there was a large body of low oxygen bottom water with the strongest hypoxia (< 62.5 μmol kg^{-1}) on the western shelf of the PRE (Figure 1), which was relatively constant among different summers of 2016 and 2019 (Figure 1). For vertical distribution, a strong salt-wedge structure was found over the inner shelf (Figures 3A, 3D) with freshwater on the shore side due to intense river discharge. Bottom waters with oxygen deficiency (< 93.5 μmol kg^{-1}) occurred below the lower boundary of the

https://doi.org/10.5194/bg-2020-243
Preprint. Discussion started: 24 July 2020

255 salt-wedge and expanded ~60 km offshore (Figure 3E). In contrast, a surface high Chl-*a* patch (6.3 μg L^{-1})
256 showed up near the upper boundary of the front, where there was enhanced water-column stability, low
257 turbidity, and high nutrients (Figures 3B, 3C). Therefore, there was a spatial mismatch between the
258 subsurface hypoxic zone (Figure 3E) and the surface chlorophyll-bloom (Figure 3F) during the
259 estuary-to-shelf transect, as both the surface Chl-*a* and oxygen right above the hypoxic zones at the bottom
260 boundary of the salt-wedge were not themselves maxima.

261 There were much higher rates of respiration (BR) and production (BP) for bulk bacterial community
262 (including FLB and PAB) in the bottom waters of X1 within the hypoxic core than those of X2 and X3
263 outside the hypoxic zone during June 2016 (Figure 4, modified from data of Xu et al., 2018). Also, the bulk
264 bacterial composition of the bottom water of X1 with 78% of α-Proteobacteria (α-Pro), 15% of
265 γ-Proteobacteria (γ-Pro), and 6% of Bacteroidetes was significantly different from those of X2 and X3
266 (91% α-Pro, 5% γ-Pro, and 2% Bacteroidetes), although their bacterial abundances were about the same
267 (Figure 4). These pointed to the importance of γ-Pro (mainly genus *Alteromonadaceae* and
268 *Pseudoalteromonaceae*) and Bacteroidetes (mainly genus *Flavobacteriaceae*) in the low-oxygen waters
269 (genus data not shown). Different taxonomic composition of bulk bacterial community for the hypoxic
270 waters was found in the 2019 cruise with on average 33% of α-Pro, 25% of γ-Pro, and 14% of
271 Bacteroidetes. In addition, relative to the bulk bacterial community of the hypoxic waters, there was
272 substantially different taxonomic composition of PAB on particles of >25 μm with 66% of γ-Pro, 22% of
273 α-Pro, and 4% of Flavobacteria.

274

275 **3.2 PUAs concentrations in the hypoxic zone**

276 Generally, there were significantly higher pPUAs (t=3.20, n=10, p<0.01) and dPUAs (t=7.61, n=8, p<0.01)
277 in the hypoxic waters than in the nearby bottom waters without hypoxia. Vertical distributions of pPUAs
278 and dPUAs in the bulk seawater were showed for two stations (Y1 and Y2) inside and outside the hypoxic
279 zone (Figure 1). Nanomolar levels of pPUAs and dPUAs were found in the water column in both stations

https://doi.org/10.5194/bg-2020-243
Preprint. Discussion started: 24 July 2020

(Figures 5E, 5F). There were high pPUAs and dPUAs in the bottom hypoxic waters of station Y1 (Figure 5E, 5F) together with locally elevated turbidity (Figure 3B) when compared to the bottom waters outside, which likely a result of particle resuspension. For station Y2 outside the hypoxia, we found negligible pPUAs and dPUAs at depths below the mixed layer (Figure 5E, 5F), which could be due to PUAs dilution by the intruded subsurface seawater.

Particle-adsorbed PUAs in the low-oxygen waters were quantified for the first time based on the particle volume estimated by large-volume-filtration (see the method section), which would reduce the uncertainty associated with particle volume calculated by empirical equations derived for marine-snow particles (Edward et al., 2015). We found high levels of particle-adsorbed PUAs (~10 μmol $L^{-1}_{particle}$) in these waters (Figure 6), which were orders of magnitude higher than the bulk water pPUAs or dPUAs concentrations (<0.3 nmol L^{-1}, Figure 5E, 5F). Particle-adsorbed PUAs of the low-oxygen waters mainly consisted of heptadienal (C7_PUA) and octadienal (C8_PUA), with decadienal (C10_PUA) making up only a small percentage.

3.3 Particle-attached bacterial growth and metabolism in the hypoxic zone

Incubation of the PAB acquired from the low-oxygen waters with direct additions of different doses of exogenous PUAs over a period of 12 hours was carried out to examine the change of bacterial growth and metabolism activities in response to PUA-enrichments. At the end of the incubation experiments, there were substantial increases of BA in both the middle and the bottom waters compared to the initial conditions for the PL treatment, while there was no difference between them for the PH treatment (Figure 7A). In particular, BA of ~$3.2 \pm 0.04 \times 10^9$ cells L^{-1} in the bottom water for the PL treatment was significantly higher (p<0.01) than the control of $2.5 \pm 0.07 \times 10^9$ cells L^{-1}.

BR was significantly promoted by the low-dose PUAs with a 21.6% increase in the middle layer (t=11.91, n=8, p<0.01) and a 25.8% increase in the bottom layer (t=11.50, n=8, p<0.01) compared to the controls. Stimulating effect of high-dose PUAs on BR was even stronger with 47.0% increase in the middle

https://doi.org/10.5194/bg-2020-243
Preprint. Discussion started: 24 July 2020

layer (t=30.56, n=8, p<0.01) and 39.8% increase in the bottom layer (t=9.40, n=8, p<0.01) (Figure 7B). Meanwhile, the cell-specific BR was significantly improved for both layers with high-dose of PUAs (p<0.05, both), but not with low-dose of PUAs (Figure 7C) due to increase of BA (Figure 7A). BGE was generally very low (<1.5%) during all the experiments (Figure 7D) due to substantially high rates of BR (Figure 7B) than BP (Figure 7E). Also, there was no significant difference in BGE between controls and PUA treatments for both layers (Figure 7D).

For the bottom layer, BP was 12.6 ± 0.8 μg C L^{-1} d^{-1} for low-dose PUAs and 16.4 ± 0.6 μg C L^{-1} d^{-1} for high-dose PUAs, which were both significantly (p<0.05 and <0.01) higher than the control of 10.6 ± 0.6 μg C L^{-1} d^{-1}. Meanwhile, BP in the middle layer was significantly higher than the control for high-dose PUAs (13.4 ± 0.9 μg C L^{-1} d^{-1}) but not for low-dose PUAs (12.6 ± 0.9 μg C L^{-1} d^{-1}) (Figure 7E). The cell-specific BP (sBP, 7.9 ± 0.5 and 6.9 ± 0.2 fg C $cell^{-1}$ d^{-1}) for high-dose PUAs were significantly (p<0.05, both) higher than the control in both layers (Figure 7F). Meanwhile, for low-dose PUAs, the sBP in both layers were not significantly different from the controls.

3.4 Particle-attached bacterial community change during incubations

Generally, γ-Pro dominated (>68%) the bacterial community at the class level for all experiments, followed by the second largest bacterial group of α-Pro. There was a large increase of γ-Pro by high-dose PUAs with increments of 17.2% and 19.5% for the middle and the bottom layers, respectively (Figure 8A), whereas there was no significant change of bacterial community composition by low-dose PUAs for both layers.

On the genus level, there was also a large difference in the responses of various bacterial subgroups to the exposure of PUAs (Figure 8B). Clearly, the main contributing genus for the promotion effect by high-dose PUAs was the group of *Alteromonas* spp., which showed a large increase in abundance by 73.9% and 69.7% in the middle and the bottom layers. For low-dose PUAs, the promotion effect of PUAs on *Alteromonas* spp. was still found although with a much lower intensity (5.4% in the middle and 19.4% in the bottom). The promotion effect of γ-Pro by high-dose PUAs was also contributed by bacteria *Halomonas*

https://doi.org/10.5194/bg-2020-243
Preprint. Discussion started: 24 July 2020

spp. (percentage increase from 1.7% to 7.4%). Meanwhile, some bacterial genus, such as *Marinobacter* and *Methylophaga* from γ-Pro, or *Nautella* and *Sulfitobacter* from α-Pro, showed decreased percentages by high-dose PUAs (Figure 8B).

3. 5 Carbon source preclusion experiments for PUAs

After one month of incubation, PAB inoculated from the low-oxygen waters showed dramatic responses to both PAH and ALK (Figure 9). In particular, the mediums of PAH addition became turbid brown (bottles on the left) with the medium of ALK addition turning into milky white (bottles in the middle) (Figures 9B and 9D), although they were both clear and transparent at the beginning of the experiments (Figures 9A and 9C). These results should reflect the growth of bacteria in these bottles with the enrichments of organic carbons. Meanwhile, the minimal medium with the addition of heptadienal (C7_PUA) remained clear and transparent as it was originally, which would indicate that PAB did not grow in the treatment of C7_PUA.

4. Discussion

Hypoxia occurs if the rate of oxygen consumption exceeds that of oxygen replenishment by diffusion, mixing, and advection (Rabouille et al., 2008). The spatial mismatch between the surface chlorophyll-*a* maxima and the subsurface hypoxia during our estuary-to-shelf transect should indicate that the low-oxygen feature may not be directly connected to particle export by the surface phytoplankton bloom. This outcome can be a combined result of riverine nutrient input in the surface, water-column stability driven by wind and buoyancy forcing, and flow convergence for an accumulation of organic matters in the bottom (Lu et al., 2018).

Elevated concentrations of pPUAs and dPUAs near the bottom boundary of the salt-wedge should reflect a sediment source of PUAs, as the surface phytoplankton above them was very low. PUA-precursors such as polyunsaturated fatty acids (PUFA) could be accumulated as detritus in the surface sediment near the PRE mouth during the spring blooms (Hu et al., 2006). Strong convergence at the bottom of the

https://doi.org/10.5194/bg-2020-243
Preprint. Discussion started: 24 July 2020

355 salt-wedge driven by shear vorticity and topography (Lu et al., 2018) would allow for resuspension of the
356 small detrital particles. Improved PUAs production by oxidation of the resuspended PUFA could occur
357 below the salt-wedge as a result of enhanced lipoxygenase activity (in the resuspended organic detritus) in
358 response to salinity increase by the intruded bottom seawater (Galeron et al., 2018).

359 Direct measurement of particle-adsorbed PUAs by large-volume filtration and on-site derivation and
360 extraction of the adsorbed PUAs yield a high level of ~10 μmol $L^{-1}_{particle}$ in the suspended particles (size
361 of >25 μm) within the hypoxic zone, which is comparable to those previously reported in sinking particles
362 of the open ocean using particle-volume calculated from diatom-derived marine snow particles (Edward et
363 al., 2015). Note that there was also a higher level of >100 μmol $L^{-1}_{particle}$ found in other stations outside the
364 PRE (unpublished data). Compared to the nanomolar levels of dPUAs and pPUAs in the water columns, a
365 micromolar level of particle-adsorbed PUAs could act as a hotspot for bacteria likely exerting important
366 impacts on microbial utilization of particulate organic matters and subsequent oxygen consumption.

367 The hypoxic waters below the salt-wedge have high turbidity probably due to particle resuspension.
368 High particle concentration here may indicate the important role of PAB, which could have a much higher
369 abundance than the FLB in the turbid waters near the mouth of the PRE (Ge et al., 2020), similar to those
370 found in the Columbia River estuary (Crump et al., 1998). Also, anaerobic bacteria and taxa preferring
371 low-oxygen conditions were found more enriched in the particle-attached communities than their
372 free-living counterparts in the PRE (Zhang et al., 2016). The respiration of PAB could take up more than
373 70% of the total bacterial respiration in the hypoxic waters (unpublished data from Dr. Bangqin Huang).
374 Therefore, it is important to address the linkage between the high-density PAB and the high level of
375 particle-adsorbed PUAs associated with the suspended particles in the low-oxygen waters.

376 Interestingly, our PUA-amended experiments for PAB retrieved from the low-oxygen waters revealed
377 distinct responses of PAB to different doses of PUAs treatments with an increase in cell growth in response
378 to low-dose PUAs (1 μmol L^{-1}) but an elevated cell-specific metabolic activity including bacterial
379 respiration and production in response to high-dose PUAs (100 μmol L^{-1}). An increase in cell density of

https://doi.org/10.5194/bg-2020-243
Preprint. Discussion started: 24 July 2020

PAB by low-dose PUAs could likely reflect the stimulating effect of PUAs on PAB growth. This finding was consistent with the previous report of a PUAs level of 0-10 μmol L^{-1} stimulating respiration and cell growth of PAB in sinking particles of the open ocean (Edwards et al., 2015). The negligible effect of low-dose PUAs on bacterial community structure in our experiments was also in good agreement with those found for PAB from sinking particles (Edwards et al., 2015). However, we do not see the inhibitory effect of 100 μmol L^{-1} PUAs on PAB respiration and production previously found in the open ocean (Edward et al., 2015). Instead, the stimulating effect for high-dose PUAs on bacterial respiration and production was even stronger with ~50% of increments. The bioactivity of PUAs on bacterial strains could likely arise from its specific arrangement of two double bonds and carbonyl chain (Ribalet et al., 2008). Our findings strongly support the important role of PUAs in enhancing bacterial oxygen utilization in the low-oxygen waters.

It is important to verify that the PUAs are not an organic carbon source but a stimulator for PAB growth and metabolism. This was supported by the fact that the inoculated PAB could not grow in the medium with 0.2 mmol L^{-1} of PUAs although they grew pretty well in the mediums with a similar amount of ALK or PAH. Our results support the previous findings that the density of *Alteromonas hispanica* was not significantly affected by 100 μmol L^{-1} of PUAs during laboratory experiments (Figure 9E), where PUAs were considered to act as cofactors for bacterial growth (Ribalet et al., 2008).

Improved cell-specific metabolism of PAB in response to high-dose PUAs was accompanied by a significant shift of bacterial community structure. The group of PAB with the greatest positive responses to exogenous PUAs was genus *Alteromonas* within the γ-Pro, which is well-known to have a particle-attached lifestyle with rapid growth response to organic matters (Ivars-Martinez et al., 2008). This result is contradicted to the previous finding of a reduced percentage of the γ-Pro class by high-dose PUAs in the PAB of open ocean sinking particles (Edward et al., 2015). Meanwhile, previous studies suggested that different genus groups within the γ-Pro may respond distinctly to PUAs (Ribalet et al., 2008). Our result was well consistent with the previous finding of the significant promotion effect of 13 or 106 μmol L^{-1}

https://doi.org/10.5194/bg-2020-243
Preprint. Discussion started: 24 July 2020

405 PUAs on *Alteromonas* (*A. hispanica* MOLA151) from the pure culture experiment (Ribalet et al., 2008). An
406 increase of PUAs could thus confer the γ-Pro (mainly *Alteromonas*) a competitive advantage over other
407 bacteria, leading to their population dominance on particles in the low-oxygen waters. These results provide
408 strong evidence for a previous hypothesis that PUAs could shape the bacterioplankton community
409 composition by driving the metabolic activity of bacteria with neutral, positive, or negative responses
410 (Balestra et al., 2011).

411 The taxonomic composition of PAB on particles of >25 μm was substantially different from that of the
412 bulk bacteria community in the hypoxic zone (with a large increase of γ-Pro associated with particles). This
413 result supports the previous report of γ-Pro being the most dominant clades attached to sinking particles in
414 the ocean (DeLong et al., 1993). A broad range of species associated with γ-Pro were known to be
415 important for quorum sensing processes due to their high population density (Doberva et al., 2015)
416 associated with sinking or suspended aggregates (Krupke et al., 2016). In particular, genus of γ-Pro such as
417 *Alteromonas* and *Pseudomonas*, are well-known quorum-sensing bacteria that can rely on diverse signaling
418 molecules to affect particle-associated bacterial communities by coordinating gene expression within the
419 bacterial populations (Long et al., 2003; Fletcher et al., 2007).

420 It has been reported that the growths of some bacterial strains of the γ-Pro such as *Alteromonas* spp.
421 and *Pseudomonas* spp. could be stimulated and regulated by oxylipins like PUAs (Ribalet et al., 2008; Pepi
422 et al., 2017). Oxylipins were found to promote biofilm formation of *Pseudomonas* spp. (Martinez et al.,
423 2016) and could serve as signaling molecules mediating cell-to-cell communication of *Pseudomonas* spp.
424 by an oxylipin-dependent quorum sensing system (Martinez et al., 2019). As PUAs are an important group
425 of chemical cues belonging to oxylipins (Franzè et al., 2018), it is thus reasonable to expect that PUAs may
426 also participate as signaling molecules for the quorum sensing among a high-density *Alteromonas* or
427 *Pseudomonas*. A high level of particle-adsorbed PUAs occurring on organic particles in the low-oxygen
428 water would thus allow particle specialists such as *Alteromonas* to regulate bacterial community structure,
429 which could alter species richness and diversity of PAB as well as their metabolic functions such as

https://doi.org/10.5194/bg-2020-243
Preprint. Discussion started: 24 July 2020

430 respiration and production when interacting with particulate organic matter in the hypoxic zone. Various
431 bacterial assemblages may have different rates and efficiencies of particulate organic matter degradation
432 (Ebrahimi et al., 2019). Coordination amongst these PAB could be critical in their ability to thrive on the
433 recycling of POC (Krupke et al., 2016) and thus directly contribute to the acceleration of oxygen
434 utilizations in the hypoxic zone. Nevertheless, the molecular mechanism of the potential PUA-dependent
435 quorum sensing of PAB may be an important topic for future study.
436
437 **5. Conclusions**
438 In summary, we found elevated concentrations of pPUAs and dPUAs in the hypoxic waters dominated by
439 PAB below the salt-wedge, together with a high level of particle-adsorbed PUAs of >10 μmol $L^{-1}_{particle}$. The
440 increase of PUAs in the bottom waters could be due to enhanced oxidation of resuspended PUFA by
441 lipoxygenase in response to increased salinity driven by seawater intrusion at the bottom of the salt-wedge.
442 We found distinct responses of PAB retrieved from the low-oxygen waters to different doses of PUAs
443 treatments with an increase of cell growth in response to low-dose PUAs (1 μmol L^{-1}) but an elevated
444 cell-specific metabolic activity including bacterial respiration and production in response to high-dose
445 PUAs (100 μmol L^{-1}). Improved cell-specific metabolism of PAB in response to high-dose PUAs was also
446 accompanied by a significant shift of bacterial community structure with increased dominance of genus
447 *Alteromonas* within the γ-Pro. Based on these observations, we hypothesize that PUAs may act as signaling
448 molecules for coordination among the high-density PAB below the salt-wedge, which allow bacteria such
449 as *Alteromonas* to thrive in degrading particulate organic matters by changing community compositions and
450 metabolic rates of PAB leading to an increase of microbial oxygen utilization that would directly contribute
451 to the formation of coastal hypoxia.
452 Our findings may be applicable to other coastal systems where there are large river inputs, intense
453 phytoplankton blooms driven by eutrophication, and strong hypoxia, such as the Chesapeake Bay, the
454 Adriatic Sea, and the Baltic Sea. For example, Chesapeake Bay is largely influenced by river runoff with

https://doi.org/10.5194/bg-2020-243
Preprint. Discussion started: 24 July 2020

455 strong eutrophication-driven hypoxia during the summer as a result of increased water stratification (Fennel
456 and Testa, 2019) and enhanced microbial respiration fueled by organic carbons produced during spring
457 diatom blooms (Harding et al., 2015). Similar to the PRE, there was also a high abundance of γ-Pro in the
458 low-oxygen waters of the Chesapeake Bay associated with the respiration of resuspended organic carbon
459 (Crump et al., 2007). Eutrophication results in intense algae bloom with phytoplankton carbon
460 sedimentation and accumulation in the coastal sediment. Oxidation of these PUFA-rich organic particles
461 during summer salt-wedge intrusion leads to high particle-adsorbed PUAs, which shifts the
462 particle-attached bacterial community to consume more oxygen when degrading particulate organic matter
463 and thus contribute to the formation of seasonal hypoxia. In this sense, the potential role of PUAs on
464 coastal hypoxia may be a byproduct of eutrophication driven by anthropogenic nutrient loading. Further
465 studies are required to quantify the contributions from PUAs-mediated oxygen loss by aerobic respiration
466 to total deoxygenation in the coastal ocean.
467
468
469 *Data availability*. Some of the data used in the present study are available in the Supplement. Other data
470 analyzed in this article are tabulated herein. For any additional data please request from the corresponding
471 author.
472
473 *Supplement*. The supplement related to this article is available online at: bg-2020-243-supplement.
474
475 *Author Contributions.* Q.P.L designed the project. Z.W. performed the experiments. Q.P.L and Z.W. wrote
476 the paper with inputs from all co-authors. All authors have given approval to the final version of the
477 manuscript.
478
479 *Competing interests.* The authors declare no competing financial interest.

https://doi.org/10.5194/bg-2020-243
Preprint. Discussion started: 24 July 2020

Acknowledgements. We are grateful to the captains and the staff of *R/V Haike68* and *R/V Tan Kah Kee* for help during the cruises. We thank Profs Dongxiao Wang (SCSIO) and Xin Liu (XMU) for organizing the cruises, Mr. Yuchen Zhang (XMU) for field assistances, Profs Changsheng Zhang (SCSIO) and Weimin Zhang (GIM) for analytical assistance, as well as Prof. Dennis Hansell (RSMAS) for critical comments.

Financial support. This work was supported by the National Key Research and Development Program of China (2016YFA0601203), the National Natural Science Foundation of China (41706181, 41676108), and the Key Special Project for Introduced Talents Team of Southern Marine Science and Engineering Guangdong Laboratory (Guangzhou) (GML2019ZD0305). ZW also wants to acknowledge a visiting fellowship (MELRS1936) from the State of Key Laboratory of Marine Environmental Science (Xiamen University).

https://doi.org/10.5194/bg-2020-243
Preprint. Discussion started: 24 July 2020

REFERENCE

Balestra, C., Alonso-Saez, L., Gasol, J. M., and Casotti, R.: Group-specific effects on coastal bacterioplankton of polyunsaturated aldehydes produced by diatoms, Aquat. Microb. Ecol., 63, 123-131, http://doi.org/10.3354/ame01486, 2011.

Breitburg, D., Levin, L. A., Oschlies, A., Gregoire, M., Chavez, F. P., Conley, D. J., Garcon, V., Gilbert, D., Gutierrez, D., Isensee, K., Jacinto, G. S., Limburg, K. E., Montes, I., Naqvi, S. W. A., Pitcher, G. C., Rabalais, N. N., Roman, M. R., Rose, K. A., Seibel, B. A., Telszewski, M., Yasuhara, M., and Zhang, J.: Declining oxygen in the global ocean and coastal waters, Science, 359, eaam7240, http://doi.org/10.1126/science.aam7240, 2018.

Crump, B. C., Peranteau, C., Beckingham, B., and Cornwell J. C.: Respiratory succession and community succession of bacterioplankton in seasonally anoxic estuarine waters, Appl. Environ. Microb., 73, 6802-6810, http://doi.org/10.1128/aem.00648-07, 2007.

Crump, B. C., Baross, J. A., and Simenstad, C. A.: Dominance of particle-attached bacteria in the Columbia River estuary, USA. Aquat. Microb. Ecol., 14, 7-18, http://doi.org/10.3354/ ame014007, 1998.

Delong, E. F., Franks, D. G., and Alldredge, A. L.: Phylogenetic diversity of aggregate-attached vs free-living marine bacterial assemblages, Limnol. Oceanogr. 38: 924-934, http://doi.org/10.4319/lo.1993.38.5.0924, 1993.

Diaz, R. J., and Rosenberg, R.: Spreading dead zones and consequences for marine ecosystems, Science, 321, 926-929, http://doi.org/10.1126/science.1156401, 2008.

Doberva, M., Sanchez-Ferandin, S., Toulza, E., Lebaron P., and Lami, R.: Diversity of quorum sensing autoinducer synthases in the Global Ocean Sampling metagenomic database, Aquat. Microb. Ecol. 74: 107-119, http://doi.org/10.3354/ame01734, 2015.

Doney, S. C., Ruckelshaus, M., Duffy, J. E., Barry, J. P., Chan, F., English, C. A., Galindo, H. M., Grebmeier, J. M., Hollowed, A. B., Knowlton, N., Polovina, J., Rabalais, N. N., Sydeman, W. J., and Talley, L. D.: Climate change impacts on marine ecosystems, Annu. Rev. Mar. Sci., 4, 11-37, http://doi.org/10.1146/annurev-marine-041911-111611, 2012.

Dyksterhouse, S. E., Gray J. P., Herwig R. P., Lara J. C. and Staley J. T.: Cycloclasticus pugetii gen. nov., sp. nov., an aromatic hydrocarbon-degrading bacterium from marine sediments, Int. J. of Syst. Bacteriol., 45: 116-123, http://doi.org/10.1099/00207713-45-1-116, 1995.

Edwards, B. R., Bidle, K. D., and van Mooy, B. A. S.: Dose-dependent regulation of microbial activity on sinking particles by polyunsaturated aldehydes: implications for the carbon cycle, P. Natl. Acad. Sci. USA., 112, 5909-5914, http://doi.org/10.1073/pnas.1422664112, 2015.

Ebrahimi, A., Schwartzman, J., and Cordero, O. X.: Cooperation and self-organization determine rate and efficiency of particulate organic matter degradation in marine bacteria, P. Natl. Acad. Sci. USA., 116, 23309-23316, http://doi.org/10.1073/pnas.1908512116, 2019.

Fennel, K., and Testa, J. M.: Biogeochemical Controls on Coastal Hypoxia, Annu. Rev. Mar. Sci., 11, 4.1-4.26, http://doi.org/10.1146/annurev-marine-010318-095138, 2019.

Fletcher, M. P., Diggle, S. P., Crusz, S. A., Chhabra, S. R., Camara, M., and Williams, P.: A dual biosensor for

https://doi.org/10.5194/bg-2020-243
Preprint. Discussion started: 24 July 2020

2-alkyl-4-quinolone quorum-sensing signal molecules, Environ. Microbiol., 9: 2683-2693, http://doi.org/10.1111/j.1462-2920.2007.01380.x, 2007.

Franzè, G., Pierson, J. J., Stoecker, D. K., and Lavrentyev, P. J.: Diatom-produced allelochemicals trigger trophic cascades in the planktonic food web, Limnol. Oceanogr., 63, 1093-1108, http://doi.org/10.1002/lno.10756, 2018.

Galeron, M. A., Radakovitch, O., Charriere, B., Vaultier, F., Volkman, J. K., Bianchi, T. S., Ward, N. D., Medeiros, P. M., Sawakuchi, H. O., Tank, S., Kerherve, P., and Rontani, J. F.: Lipoxygenase-induced autoxidative degradation of terrestrial particulate organic matter in estuaries: A widespread process enhanced at high and low latitude, Org. Geochem., 115, 78-92, http://doi.org/10.1016/j.orggeochem.2017.10.013, 2018.

Garneau, M.E., Vincent, W.F., Terrado, R., and Lovejoy, C.: Importance of particle-associated bacterial heterotrophy in a coastal Arctic ecosystem, J. Marine Syst., 75, 185-197, http://doi.org/10.1016/j.jmarsys.2008.09.002, 2009.

Ge, Z., Wu, Z., Liu Z., Zhou, W., Dong, Y., and Li, Q. P.: Using detaching method to determine the abundance of particle-attached bacteria from the Pearl River Estuary and its coupling relationship with environmental factors, Chinese J. Mar. Environ. Sci., http://doi.org/ 10.12111/j.mes.20190065, 2020.

Harding, Jr. L. W., , Adolf, J. E., Mallonee, M. E., Miller, W. D., Gallegos, C. L., Perry, E. S., Johnson, J. M., Sellner, K. G., and Paerl H. W.: Climate effects on phytoplankton floral composition in Chesapeake Bay, Estuar. Coast. Shelf S., 162, 53-68, http://doi.org/10.1016/ j.ecss.2014.12.030, 2015.

He, B. Dai, M., Zhai, W., Guo, X., and Wang, L.: Hypoxia in the upper reaches of the Pearl River Estuary and its maintenance mechanisms: A synthesis based on multiple year observations during 2000-2008, Mar. Chem., 167, 13-24, http://doi.org/10.1016/j.marchem.2014.07.003, 2014.

Hopkinson, C.S.: Shallow-water benthic and pelagic metabolism- evidence of heterotrophy in the nearshore Geogia bight, Mar. Biol., 87, 19-32, http://doi.org/10.1007/bf00397002, 1985.

Helm, K. P., Bindoff, N. L., and Church, J. A.: Observed decreases in oxygen content of the global ocean, Geophys. Res. Lett., 38, L23602. http://doi.org/10.1029/2011GL049513, 2011.

Hmelo, L. R., Mincer, T. J., and Van Mooy, B. A. S.: Possible influence of bacterial quorum sensing on the hydrolysis of sinking particulate organic carbon in marine environments, Env. Microbiol. Rep., 3, 682-688, http://doi.org/10.1111/j.1758-2229.2011.00281.x, 2011.

Huang, Y., Liu, X., Laws, E. A., Chen, B., Li, Y., Xie, Y., Wu, Y., Gao, K., and Huang, B.: Effects of increasing atmospheric CO_2 on the marine phytoplankton and bacterial metabolism during a bloom: A coastal mesocosm study, Sci. Total Environ., 633, 618-629, http://doi.org/10.1016/j.scitotenv.2018.03.222, 2018.

Hu, J., Zhang H., and Peng P.: Fatty acid composition of surface sediments in the subtropical Pearl River estuary and adjacent shelf, Southern China. Estuar. Coast, Shelf S., 66: 346-356, http://doi.org/10.1016/j.ecss.2005.09.009, 2006.

Ianora, A., and Miralto, A.: Toxigenic effects of diatoms on grazers, phytoplankton and other microbes: a review, Ecotoxicology, 19, 493-511, http://doi.org/10.1007/s10646-009-0434-y, 2010.

Ivars-Martinez, E., Martin-Cuadrado, A. B., D'Auria, G., Mira, A., Ferriera, S., Johnson, J., et al.: Comparative

https://doi.org/10.5194/bg-2020-243
Preprint. Discussion started: 24 July 2020

564 genomics of two ecotypes of the marine planktonic copiotroph *Alteromonas macleodii* suggests alternative
565 lifestyles associated with different kinds of particulate organic matter. ISME, J2, 1194–1212, 2008.
566 Kemp, W. M., Testa, J. M., Conley, D. J., Gilbert, D., and Hagy, J. D.: Temporal responses of coastal hypoxia to
567 nutrient loading and physical controls, Biogeosciences, 6, 2985-3008, http://doi.org/10.5194/bg-6-2985-2009,
568 2009.
569 Krupke, A., Hmelo, L. R., Ossolinski, J. E., Mincer, T. J., and Van Mooy, B. A. S.: Quorum sensing plays a complex
570 role in regulating the enzyme hydrolysis activity of microbes associated with sinking particles in the ocean,
571 Front. Mar. Sci., 3:55, http://doi.org/10.3389/fmars. 2016.00055, 2016.
572 Kirchman D. L.: Leucine incorporation as a measure of biomass production by heterotrophic bacteria, in: Hand book
573 of methods in aquatic microbial ecology, edited by: Kemp, P. F., Cole, J. J., Sherr, B. F., and Sherr, E. B., Lewis
574 Publishers, Boca Raton, 509–512, http://doi.org/10.1201/9780203752746-59, 1993.
575 Long, R. A., Qureshi, A., Faulkner, D. J., and Azam, F.: 2-n-pentyl-4-quinolinol produced by a marine Alteromonas
576 sp and its potential ecological and biogeochemical roles, Appl. Environ. Microb., 69, 568-576,
577 http://doi.org/10.1128/aem.69.1.568-576.2003, 2003.
578 Lu, Z., Gan, J., Dai, M., Liu, H., and Zhao, X.: Joint effects of extrinsic biophysical fluxes and intrinsic
579 hydrodynamics on the formation of hypoxia west off the Pearl River Estuary, J. Geophys. Res.-Oceans., 123,
580 https://doi.org/10.1029/2018JC014199, 2018.
581 Lunau, M., Lemke, A., Walther, K., Martens-Habbena, W., and Simon, M.: An improved method for counting
582 bacteria from sediments and turbid environments by epifluorescence microscopy, Environ. Microbiol., 7,
583 961-968, http://doi.org/10.1111/j.1462-2920.2005.00767.x, 2005.
584 Martinez, E., and Campos-Gomez, J.: Oxylipins produced by Pseudomonas aeruginosa promote biofilm formation
585 and virulence, Nat. Commun., 7, 13823, https://doi.org/10.1038/ncomms13823, 2016.
586 Martinez, E., Cosnahan, R. K., Wu, M. S., Gadila, S. K., Quick, E. B., Mobley, J. A., and Campos-Gomez, J.:
587 Oxylipins mediate cell-to-cell communication in Pseudomonas aeruginosa, Commun. Biol., 2, 66,
588 https://doi.org/10.1038/s42003-019-0310-0, 2019.
589 Oudot, C., Gerard, R., Morin, P., and Gningue, I.: Precise shipboard determination of dissolved-oxygen (winkler
590 procedure) for productivity studies with a commercial system, Limnol. Oceanogr., 33, 146-150,
591 http://doi.org/10.4319/lo.1988.33.1.0146, 1988.
592 Parsons, T. R., Maita, Y., and Lalli, C. M.: Fluorometric Determination of Chlorophylls, in: A manual of chemical
593 and biological methods for seawater analysis, Pergamum Press, Oxford, 107-109,
594 http://doi.org/10.1016/B978-0-08-030287-4.50034-7, 1984.
595 Pepi, M., Heipieper, H. J., Balestra, C., Borra, M., Biffali, E., and Casotti, R.: Toxicity of diatom polyunsaturated
596 aldehydes to marine bacterial isolates reveals their mode of action, Chemosphere, 177, 258-265, 2017
597 Rabouille, C., Conley, D. J., Dai, M. H., Cai, W. J., Chen, C. T. A., Lansard, B., Green, R., Yin, K., Harrison, P. J.,
598 Dagg, M., and McKee, B.: Comparison of hypoxia among four river-dominated ocean margins: The Changjiang
599 (Yangtze), Mississippi, Pearl, and Rhone rivers, Cont. Shelf Res., 28, 1527-1537,

https://doi.org/10.5194/bg-2020-243
Preprint. Discussion started: 24 July 2020

600 http://doi.org/10.1016/j.csr.2008.01.020, 2008.
601 Ribalet, F., Intertaglia, L., Lebaron, P., and Casotti, R.: Differential effect of three polyunsaturated aldehydes on
602 marine bacterial isolates, Aquat. Toxicol., 86, 249-255, http://doi.org/10.1016/j.aquatox.2007.11.005, 2008.
603 Su, J., Dai, M., He, B., Wang, L., Gan, J., Guo, X., Zhao, H., and Yu, F.: Tracing the origin of the oxygen-consuming
604 organic matter in the hypoxic zone in a large eutrophic estuary: the lower reach of the Pearl River Estuary, China,
605 Biogeosciences, 14, 4085-4099, http://doi.org/10.5194/bg-14-4085-2017, 2017.
606 Wang, N., Lin, W., Chen, B., and Huang, B.: Metabolic states of the Taiwan Strait and the northern South China Sea
607 in summer 2012, J. Trop. Oceanogr., 33, 61-68, http://doi.org/doi:10.3969/j.issn.1009-5470.2014.04.008, 2014.
608 Williams, P. J. I. and de Giorgio, P. A.: Respiration in Aquatic Ecosystems: history and background, in: Respiration in
609 Aquatic Ecosystems, edited by de Giorgio, P. A., and Williams, P. J. I., Oxford University Press, New York, 1-17,
610 http://doi.org/10.1093/acprof:oso/ 9780198527084.003.0001, 2005.
611 Wu, Z., and Li, Q. P.: Spatial distributions of polyunsaturated aldehydes and their biogeochemical implications in the
612 Pearl River Estuary and the adjacent northern South China Sea, Prog. Oceanogr., 147, 1-9,
613 http://doi.org/10.1016/j.pocean.2016.07.010, 2016.
614 Xu, J., Li, X., Shi, Z., Li, R., and Li, Q. P.: Bacterial carbon cycling in the river plume in the northern South China
615 Sea during summer, J. Geophys. Res.-Oceans, 123, 8106-8121, http://doi.org/10.1029/2018jc014277, 2018.
616 Yin, K., Lin, Z., and Ke, Z.: Temporal and spatial distribution of dissolved oxygen in the Pearl River Estuary and
617 adjacent coastal waters, Cont. Shelf Res., 24, 1935-1948, http://doi.org/10.1016/j.csr.2004.06.017, 2004.
618 Zhang, H., and Li, S.: Effects of physical and biochemical processes on the dissolved oxygen budget for the Pearl
619 River Estuary during summer, J. Marine Syst., 79, 65-88, http://doi.org/10.1016/j.jmarsys.2009.07.002, 2010.
620 Zhang, Y., Xiao, W., and Jiao, N.: Linking biochemical properties of particles to particle-attached and free-living
621 bacterial community structure along the particle density gradient from freshwater to open ocean, J. Geophys.
622 Res.-Biogeo., 121, 2261-2274, http://doi.org/10.1002/2016jg003390, 2016.

https://doi.org/10.5194/bg-2020-243
Preprint. Discussion started: 24 July 2020

623 **Table 1**. Summary of treatments in the experiments of exogenous PUAs additions for the low-oxygen
624 waters at station Y1 during June 2019. The PUAs solution includes heptadienal (C7_PUA), octadienal
625 (C8_PUA), and decadienal (C10_PUA) with the mole ratios of 10:1:10.
626

		Treatment
1	Control (methanol)	400 μL of methanol
2	Low-dose PUAs (methanol)	400 μL of 2 mM PUAs in methanol
3	High-dose PUAs (methanol)	400 μL of 200 mM PUAs in methanol

627
628

https://doi.org/10.5194/bg-2020-243
Preprint. Discussion started: 24 July 2020

Figures and Legends

Figure 1: Sampling map of the Pearl River Estuary and the adjacent northern South China Sea during (A) June 17th-28th, 2016, (B) June 18st-June 2nd, 2019. Contour shows the bottom oxygen distribution with white lines highlighting the levels of 93.5 μmol kg^{-1} (oxygen-deficient zone) and 62.5 μmol kg^{-1} (hypoxic zone); dashed line in panel A is an estuary-to-shelf transect with red dots for three stations with bacterial metabolic rate measurements; diamonds in panel B are two stations with vertical pPUAs and dPUAs measurements with Y1 the station for PUAs-amended experiments.

Figure 2: Procedure of large-volume filtration and subsequent experiments. A large volume of the low-oxygen water was filtered through a 25-μm filter to obtain the particles-adsorbed PUAs and the particle-attached bacteria (PAB). The carbon-source test of PUA for the inoculated PAB includes the additions of PUA, alkanes (ALK), and polycyclic aromatic hydrocarbons (PAH). PUAs-amended experiments for PAB include Control (CT), Low-dose (PL), and High-dose PUAs (PH). Samples in the biological oxygen demand (BOD) bottles at the end of the experiment were analyses for bacterial respiration (BR), abundances (BA), production (BP) as well as DNA. Note that pPUAs and dPUAs are particulate and dissolved PUAs in the seawater.

Figure 3: Vertical distributions of (A) temperature, (B) turbidity, (C) nitrate, (D) salinity, (E) dissolved oxygen, and (F) chlorophyll-*a* from the estuary to the shelf of the NSCS during June 2016. Section locations are shown in Figure 1; the white line in panel D shows the area of oxygen deficiency zone (<93.5 μmol kg^{-1}).

Figure 4: Comparisons of oxygen, bulk bacterial respiration (BR) and production (BP), as well as bulk bacterial abundances (BA) of α-Proteobacteria (α-Pro), γ-Proteobacteria (γ-Pro), Bacteroidetes (Bact), and other bacteria for the bottom waters between stations inside (X1) and outside (X2 and X3) the hypoxic zone during the 2016 cruise. Bulk bacteria community includes FLB and PAB of <20 μm. Locations of stations X1, X2, X3 are showed in Figure 1A.

Figure 5: Vertical distributions of (A) temperature, (B) salinity, (C) dissolved oxygen (DO), (D) chlorophyll-*a* (Chl-*a*), (E) particulate PUAs (pPUAs) and (F) dissolved PUAs (dPUAs) inside (Y1) and outside (Y2) the hypoxic zone during June 2019. Locations of station Y1 and Y2 are shown in Figure 1.

Figure 6: Concentrations of particle-adsorbed PUAs (in micromoles per liter particle) in the middle and the

https://doi.org/10.5194/bg-2020-243
Preprint. Discussion started: 24 July 2020

662 bottom waters of station Y1 during June 2019. Three different PUA components are also shown including
663 heptadienal (C7_PUA), octadienal (C8_PUA), and decadienal (C10_PUA).
664
665 **Figure 7:** Responses of particle-attached bacterial parameters including (A) bacterial abundance ($BA_{particle}$),
666 (B) bacterial respiration ($BR_{particle}$), (C) cell-specific bacterial respiration ($sBR_{particle}$), (D) bacterial growth
667 efficiency ($BGE_{particle}$), (E) bacterial production ($BP_{particle}$), and (F) cell-specific bacterial production
668 ($sBP_{particle}$) to different doses of PUAs additions at the end of the experiments for the middle (12 m) and the
669 bottom waters (25 m) at station Y1. Error bars are standard deviations (n = 3 or 4). The star represents a
670 significant difference (p<0.05) with PL and PH the low and high dose PUA treatments and C the control.
671
672 **Figure 8:** Variation of particle-attached bacterial community compositions on (A) the phylum level and (B)
673 the genus level in response to different doses of PUAs additions at the end of the experiments for the
674 middle and the bottom waters at station Y1. Labels PL and PH are for the low- and high-dose PUAs with
675 CT the control.
676
677 **Figure 9:** Carbon-source test of PUAs with cell culture of particle-attached bacteria inoculated from the
678 low-oxygen waters of station Y1 including the initial conditions (Day0) at the beginning of the experiments
679 as well as results after 30 days of incubations (Day30) for (A, B) the middle and (C, D) the bottom waters,
680 respectively. Bottles from left to right are the mediums (M) with the additions of polycyclic aromatic
681 hydrocarbons (M+PAH, 200 ppm), alkanes (M+ALK, 0.25 g L^{-1}), and heptadienal (M+C7_PUA, 0.2 mmol
682 L^{-1}); Note that a change of turbidity should indicate bacterial utilization of organic carbons. (E) the optical
683 density of bacterium *Alteromonas hispanica* MOLA151 growing in the minimal medium as well as in the
684 mediums with the additions of mannitol, pyruvate, and proline (M+MPP, 1% each,), heptadienal
685 (M+C7_PUA, 145μM), octadienal (M+C8_PUA, 130μM,), and decadienal (M+C10_PUA, 106μM). data
686 of panel D are reproduced from Ribalet et al., 2008.

https://doi.org/10.5194/bg-2020-243
Preprint. Discussion started: 24 July 2020

Biogeosciences
Discussions
Open Access
EGU

687

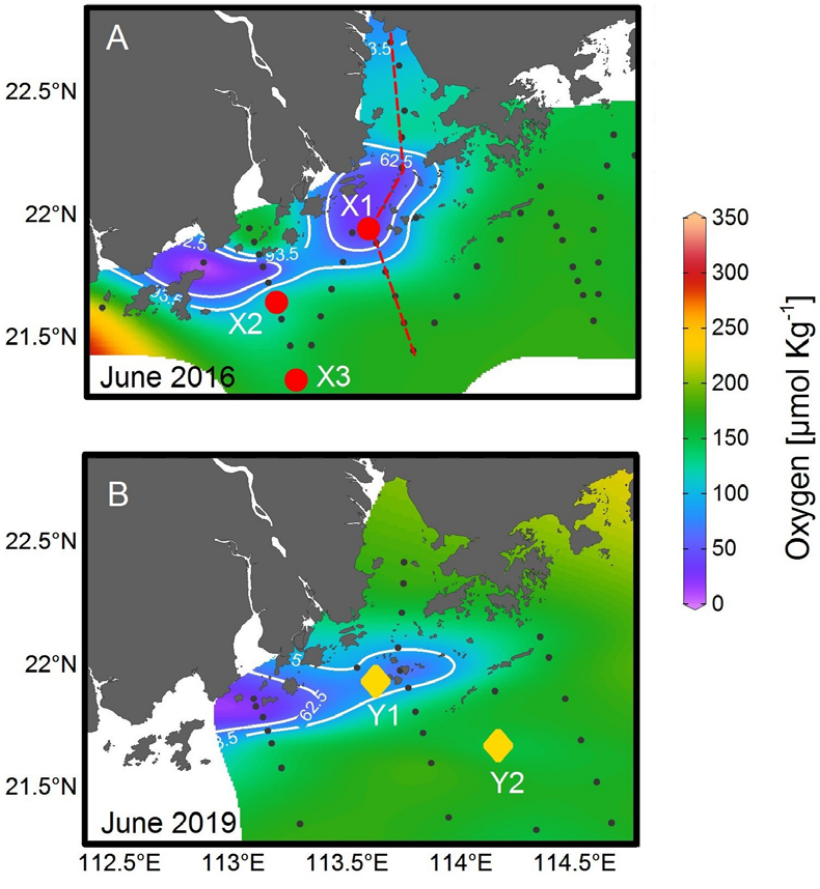

688

689

690 **Figure 1**

691

https://doi.org/10.5194/bg-2020-243
Preprint. Discussion started: 24 July 2020

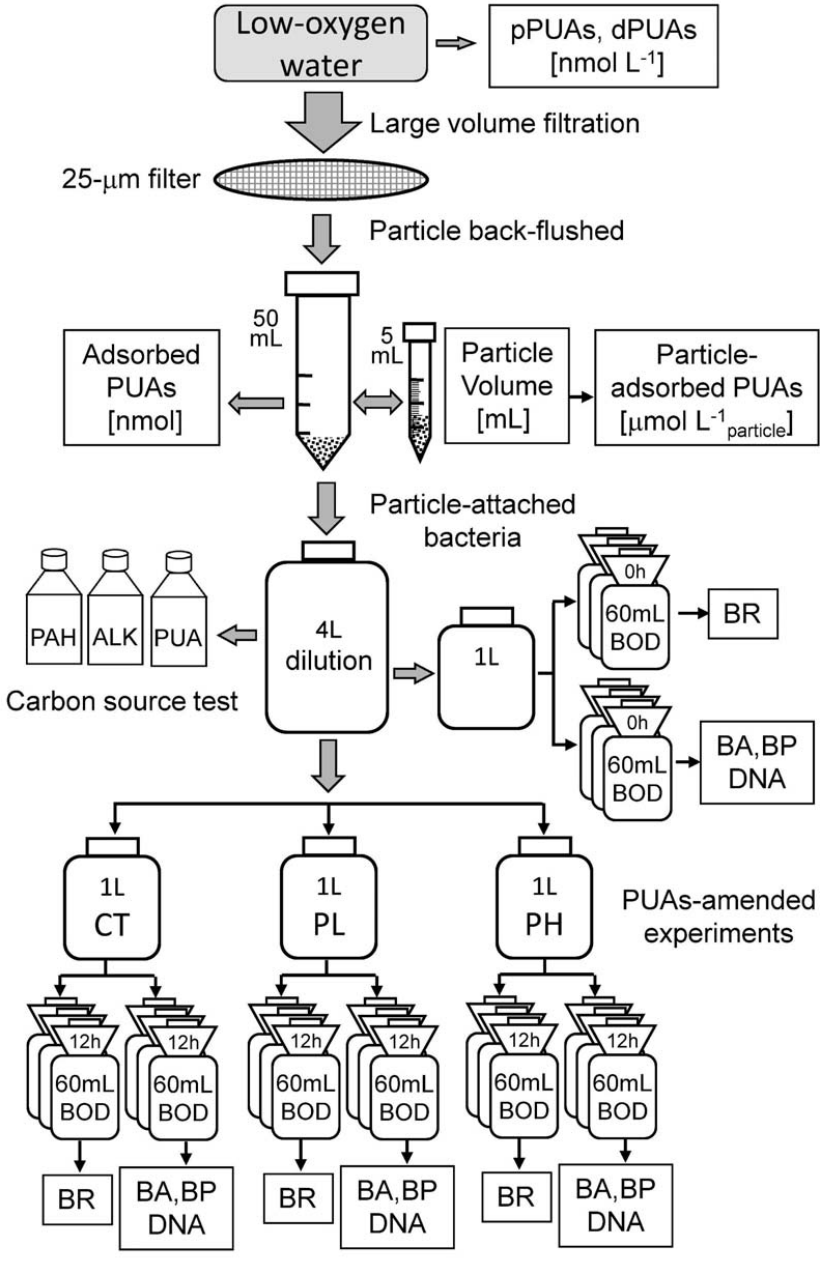

692

693 **Figure 2**

https://doi.org/10.5194/bg-2020-243
Preprint. Discussion started: 24 July 2020

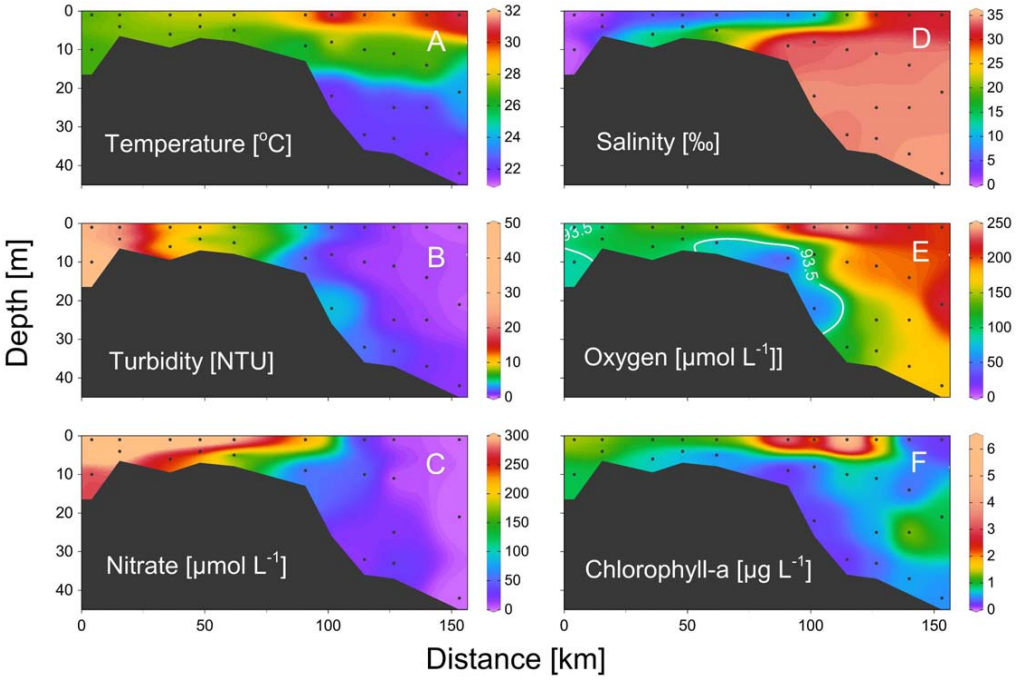

694
695
696

Figure 3

https://doi.org/10.5194/bg-2020-243
Preprint. Discussion started: 24 July 2020

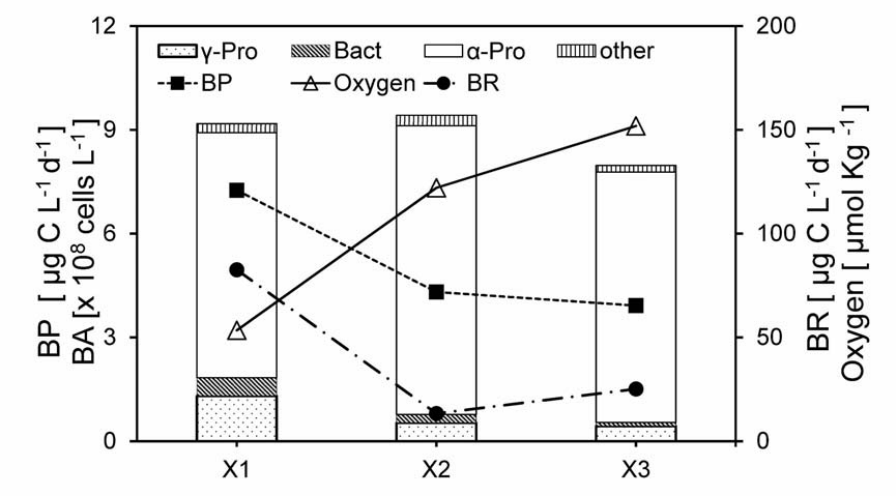

Figure 4

https://doi.org/10.5194/bg-2020-243
Preprint. Discussion started: 24 July 2020

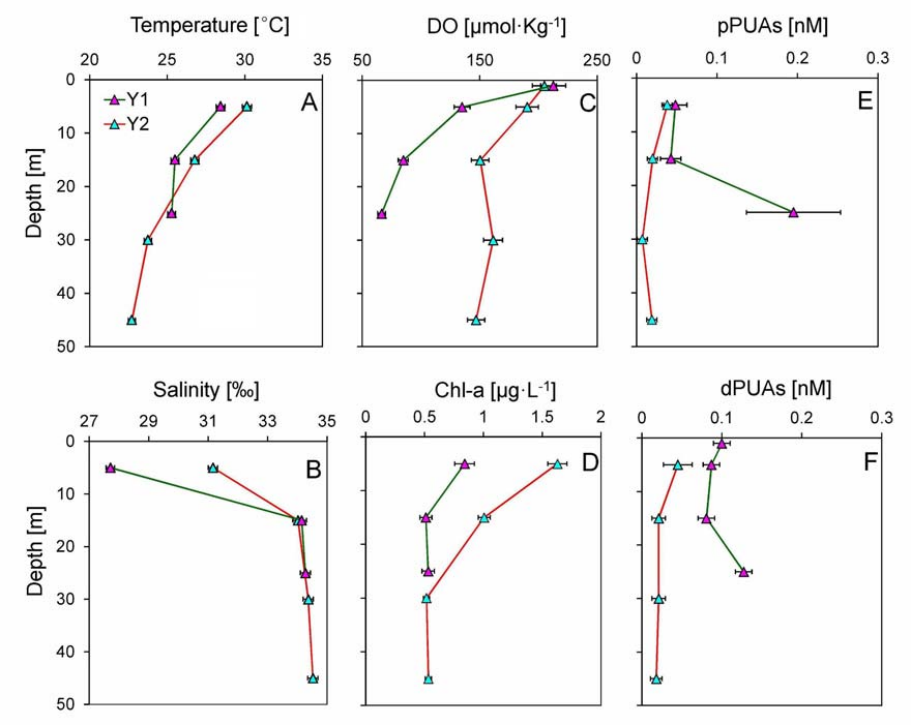

Figure 5

https://doi.org/10.5194/bg-2020-243
Preprint. Discussion started: 24 July 2020

Biogeosciences
Discussions
Open Access
EGU

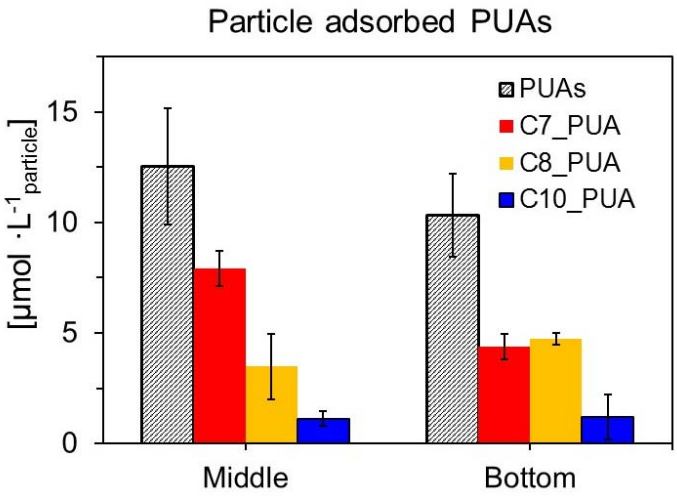

705
706
707 **Figure 6**
708

https://doi.org/10.5194/bg-2020-243
Preprint. Discussion started: 24 July 2020

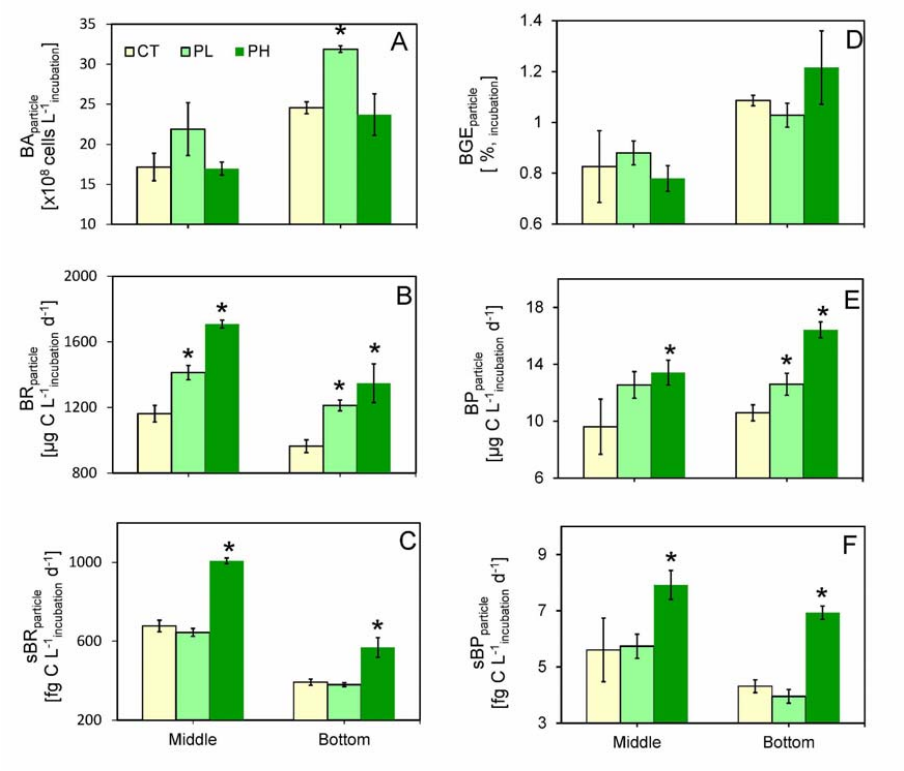

Figure 7

https://doi.org/10.5194/bg-2020-243
Preprint. Discussion started: 24 July 2020

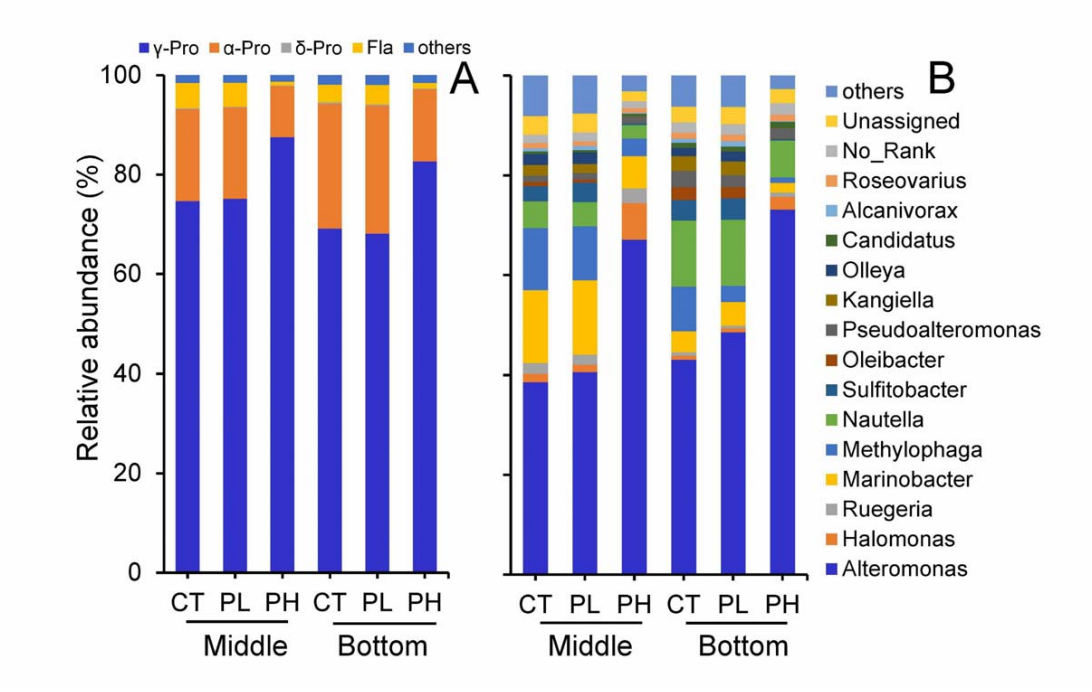

713
714
715

Figure 8

https://doi.org/10.5194/bg-2020-243
Preprint. Discussion started: 24 July 2020

Biogeosciences
Discussions
Open Access
EGU

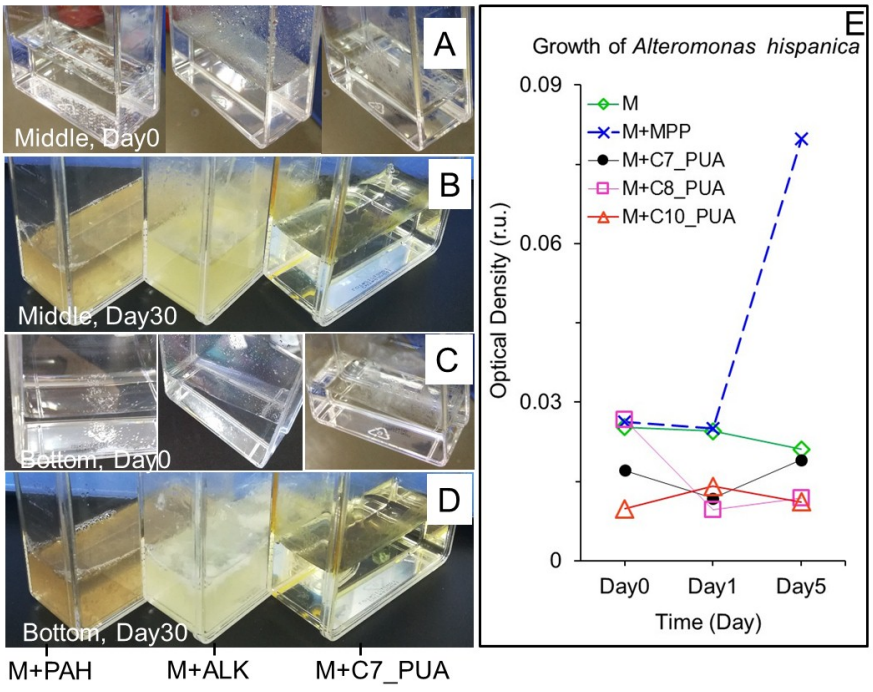

716
717
718 **Figure 9**
719